FEBS Letters 532 (2002) 36–44 FEBS 26744

HIV-1 TAT-mediated protein transduction and subcellular localization using novel expression vectors[1]

Yonghui Yang, Jun Ma, Zhiyin Song, Mian Wu*

Department of Molecular and Cellular Biology and Key Laboratory of Structural Biology, School of Life Sciences, University of Science and Technology of China, Hefei, Anhui 230026, PR China

Received 5 July 2002; revised 15 October 2002; accepted 17 October 2002

First published online 1 November 2002

Edited by Hans-Dieter Klenk

Abstract **Several novel prokaryotic and eukaryotic expression vectors were constructed for protein transduction and subcellular localization. These vectors employed an N-terminal stretch of 11 basic amino acid residues (47–57) from the human immunodeficiency virus type 1 (HIV-1) TAT protein transduction domain (PTD) for protein translocation and cellular localization. The vectors also contained a six-histidine (His_6) tag at the N- or C-terminus for convenient purification and detection, and a multiple cloning site for easy insertion of foreign genes. Some heterologous genes including HSV-TK, Bcl-rambo, Smac/DIABLO and GFP were fused in-frame to TAT PTD and successfully overexpressed in *Escherichia coli*. The purified TAT-GFP fusion protein was able to transduce into the mammalian cells and was found to locate mainly in the cytosol when exogenously added to the cell culture medium. However, using a transfection system, mammalian-expressed TAT-GFP predominantly displayed a nuclear localization and nucleolar accumulation in mammalian cell lines. This discrepancy implies that the exact subcellular localization of transduced protein may depend on cell type, the nature of imported proteins and delivery approach. Taken together, our results demonstrate that a TAT PTD length of 11 amino acids was sufficient to confer protein internalization and its subsequent cellular localization. These novel properties allow these vectors to be useful for studying protein transduction and nuclear import.**

Key words: Human immunodeficiency virus type 1 TAT; Protein transduction domain; Nuclear localization signal

1. Introduction

Efficient intracellular delivery and correct localization of pharmaceutical macromolecules remains problematic because of the barrier of impermeable cell membranes. In 1988, however, Green and Frankel independently discovered that human immunodeficiency virus type 1 (HIV-1)-encoded *trans*-activator TAT protein, an 86-amino acid protein which is essential for viral gene expression and replication, could rapidly enter cells, even the nucleus, and subsequently *trans*-activate the viral long terminal repeat promoter when added exogenously to the culture medium [1,2]. From then on, increasing evidence has shown that TAT protein is capable of mediating heterologous proteins across the plasma membrane into nearly all eukaryotic cells [3]. This unique transport mode is not receptor-, transporter-, or endocytosis-dependent, rather it is concentration-dependent [4]. Thus far, the exact mechanism by which TAT-linked proteins can freely enter cells still remains unclear. Nevertheless, several other proteins with a protein transduction domain (PTD), including ANTP from *Drosophila* and VP22 from herpes simplex virus (HSV), have been identified [5]. Previous studies have shown that the 11-amino acid TAT peptide YG**RKKRRQRRR** (residues 47–57), rich in basic amino acids (highlighted in bold), is sufficient for intracellular transduction and subcellular localization [6,7]. It is believed that this short TAT motif can functionally be dissected into two parts: GRKKR can act as a potential nuclear localization signal (NLS), whereas RRR appears to be very critical for protein translocation [6]. Recently, Dowdy's group have conducted many pioneer researches in this field and have developed the bacterial expression vector pTAT/TAT-HA for this purpose [7]. In addition, using a transfection system and indirect immunofluorescence analysis, Ruben et al. [8] and Hauber et al. [9] reported that TAT protein was localized predominantly in the nucleus, with accumulation especially within the nucleolus. The enhanced green fluorescent protein (GFP) is widely used as a marker for monitoring gene expression and cellular localization; we therefore employed this fluorescent protein to generate TAT-GFP fusion protein to address the intracellular transduction and subcellular location of TAT PTD in mammalian cells.

In order to facilitate the investigation of the mechanism of TAT-mediated protein delivery into cells and subsequent subcellular localization, we developed several novel prokaryotic and eukaryotic expression vectors, in which an 11-amino acid HIV-1 TAT PTD or a TAT PTD mutant (TAT-m) with six amino acid substitutions within the TAT peptide, YARAAARQARA, was included [10]. The HSV thymidine kinase (TK) gene, the enhanced GFP gene and two mammalian pro-apoptotic genes, Bcl-rambo [11] and Smac/DIABLO [12,13], were tested for their overproduction in *Escherichia coli*. Bacterially expressed TAT-Smac/DIABLO and TAT-GFP could be successfully taken up by the target cells. It is interesting to note that the imported TAT-Smac/DIABLO did not appear to localize in the cytosol, whereas the TAT-GFP was largely observed in the cytosol when exogenously added to the cultured cells. Using a transfection system, however, TAT-GFP was showed to localize mainly in the nucleus and accumulate

*Corresponding author. Fax: (86)-551-3606264.
E-mail address: wumian88@yahoo.com (M. Wu).

[1] The nucleotide sequences of vectors pETAT-1/2/11/12, pNB-3/13, pHis-TAT-GFP, pHis-TAT-m-GFP and pHis-GFP have been deposited in GenBank under accession numbers AF525441–525449.

0014-5793/02/$22.00
PII: S0014-5793(02)03624-4

in the nucleolus in all mammalian cells tested. In contrast to TAT PTD, mutant TAT-m completely abolished its nuclear localization.

2. Materials and methods

2.1. Oligonucleotides

All primers used in this study are listed as follows. Restriction enzyme sites incorporated to facilitate cloning are underlined. P_{nkb-1} 5′-AACATATGTACGGTCGTAAAAAACGTCGTCAGCGTCGT-CGTGGTACCATGGCTTCGTACCCCTGCCA-3′ (*Nde*I, *Kpn*I), P_{nkb-2} 5′-AACATATGTACGCTCGTGCTGCTGCTCGTCAGGC-TCGTGCTGGTACCATGGCTTCGTACCCCTGCCA-3′ (*Nde*I, *Kpn*I), P_{nkb-3} 5′-AACATATGGGTACCATGGCTTCGTACCCCT-GCCA-3′ (*Nde*I, *Kpn*I), P_{nkb-4} 5′-CGGGATCCGAGGTACCGTG-AGCCTCCCCCATCTCCC-3′ (*Bam*HI, *Kpn*I), P_{tk-1} 5′-GAA-GATCTGCCACCATGGGCAGCAGCCAT-3′ (*Bgl*II) and P_{tk-2} 5′-CCGCTCGAGGGTACCTCAGTGAGCCTCCCCCATCTC-3′ (*Xho*I, *Kpn*I).

2.2. Construction of vectors

pET-22b(+), pET-15b (Novagen) and pEGFP-N1 (Clontech) were the parental plasmids for construction of various prokaryotic and eukaryotic expression vectors. Using plasmid pAdbm5-TK bearing the HSV-TK gene as a template, primer pairs P_{nkb-1}/P_{nkb-4}, P_{nkb-2}/P_{nkb-4} and P_{nkb-3}/P_{nkb-4} were used for amplification of the TAT-TK, TAT-m-TK and TK gene fragments respectively. The three resultant PCR products were digested with *Nde*I/*Bam*HI and subcloned into pET-22b(+) to generate plasmids named pNKB-1, pNKB-2 and pNKB-3. These plasmids were digested with *Nde*I and *Xho*I, and the smaller segments containing the TAT-TK, TAT-m-TK and TK coding regions were ligated into pET-15b to create pNKB-11, pNKB-12 and pNKB-13. These six plasmids were cleaved with *Kpn*I to remove the TK gene, and the resultant larger fragments were self-religated to yield six different vectors designated pETAT-1, pETAT-2 and pNB-3 (pET-22b(+)-based) and pETAT-11, pETAT-12 and pNB-13 (pET-15b-based). To generate eukaryotic expression vectors, we designed two primers P_{tk-1} and P_{tk-2}. Forward primer P_{tk-1} corresponded to the region upstream of the six-histidine (His_6) tag with which three bases were overlapping and reverse primer P_{tk-2} was made to complement the 3′ region of the HSV-TK gene. Using pNKB-11, pNKB-12 and pNKB-13 as templates, we successfully amplified three PCR products, which were then digested and subcloned into the *Bgl*II and *Xho*I sites of pAdTrack-CMV [14] to generate plasmids pAd/His-TAT-TK, pAd/His-TAT-m-TK and pAd/His-TK. The resultant recombinant plasmids were further digested with *Kpn*I to remove the HSV-TK gene, and self-religated again to yield pAd/His-TAT, pAd/His-TAT-m and pAd/His. The smaller *Bgl*II- and *Xho*I-digested fragments released from these plasmids were inserted into the same sites of pEGFP-N1 to generate pHis-TAT-GFP, pHis-TAT-m-GFP and pHis-GFP. The nucleotide sequences of all PCR products were confirmed by the ABI Prism automated sequencing method.

2.3. Expression and purification of TAT fusion proteins

The recombinant prokaryotic plasmids were transformed into *E. coli* strain BL21 (DE3) to express fusion proteins with or without TAT PTD. The bacteria were grown to reach an OD_{600} of approximately 0.5–0.8 prior to induction. For expression of TAT-TK, TAT-Bcl-rambo and TAT-GFP, cells were induced with 1 mM isopropyl-β-D-thiogalactoside (IPTG) for 3–6 h, for expression of TAT-Smac, cells were induced with 0.1 mM IPTG for 6 h. The cells were then harvested, suspended in binding buffer (20 mM Tris–HCl, pH7.9, 0.5 M NaCl) and sonicated. The solubilized TAT-Smac fusion protein was purified under native conditions, and TAT-GFP was purified under denatured and native conditions respectively. To denature TAT-GFP fusion protein, the harvested cells were sonicated in binding buffer containing 8 M urea. The fusion proteins were purified by Ni^{2+} affinity chromatography using a chelating Sepharose resin column (Pharmacia). After the column was washed with 100 mM imidazole in binding buffer, the fusion protein was eluted with 1 M imidazole in binding buffer. The fusion protein in either native or denatured form was then concentrated, desalted and buffer exchanged to phosphate-buffered saline (PBS) using a stirred ultrafiltration cell (Millipore), the purified fusion protein could be used directly for protein transduction or aliquoted and stored frozen in 10% glycerol at −80°C [15,16].

For the transduction of TAT fusion proteins, cells were cultured to 70–80% confluence in 24-well microtiter plates. Just before transduction, the culture media were removed and replaced by 0.5 ml fresh medium, to which TAT fusion proteins at various concentrations were then added. After incubation for indicated intervals, the cells were washed with PBS at least four to five times to avoid possible aggregation of proteins. Cells were then examined directly by fluorescence microscopy and further used for Western blot analysis.

2.4. Cell death assay

The MTT assay was used to determine cell viability. Briefly, A549 cells were plated at 1×10^4cells/well in 96-well microtiter plates and incubated overnight. After replacement with fresh medium, cells were treated with TAT-Smac or Smac at final concentrations of 100 nM, 200 nM and 400 nM for 6 h. Taxol was added to the media at a final concentration of 100 nM and incubated for another 10 h followed by addition of 10 μl of 5 mg/ml MTT solution. After incubation, the media were removed and replaced with 100 μl dimethyl sulfoxide and the data were analyzed using an EL_X800 Universal Microplate Reader (Bio-Tek Instruments) at a wavelength of 570 nm. The effect of cell death was normalized as a percentage using cells treated with taxol alone as control.

2.5. Cell cultures and transfections

Human glioblastoma cell line A172, human embryonic kidney cell line 293T, human cervical cancer cell line HeLa and monkey kidney cell line COS-7 were cultured in Dulbecco's modified Eagle's medium supplemented with 10% fetal bovine serum (FBS) and antibiotics penicillin (100 U/ml)/streptomycin (0.1 mg/ml) at 37°C in 5% CO_2. Human lung carcinoma cell line A549 and rat glioma cell line C6 were grown in RPMI 1640 medium containing 10% fetal calf serum (FCS) and penicillin (100 U/ml)/streptomycin (0.1 mg/ml) and maintained at 37°C/5% CO_2. Transfections of cells were performed using Lipofectamine 2000 (Invitrogen) according to the manufacturer's specifications.

2.6. Western blot analysis

Western blot was carried out mainly according to the manufacturer's instructions. Briefly, cells were harvested, washed twice with cold PBS (pH 7.4) and then resuspended in lysis buffer (50 mM Tris–HCl (pH 7.5), 250 mM NaCl, 5 mM EDTA, 50 mM NaF, 0.5% NP-40) supplemented with protease inhibitor cocktail (Roche) on ice for 30 min. The lysate was centrifuged, and supernatants and pellets were mixed with an equal volume of 2× Laemmli's buffer respectively. The samples were loaded and separated by 12% SDS–polyacrylamide gel. The resolved proteins were transferred onto a nitrocellulose membrane (Amersham). The blot was blocked with 5% milk in Tris-buffered saline+Tween (TBST) and then incubated with mouse anti-GFP polyclonal antibody (Clontech) or anti-His polyclonal antibody (Santa Cruz) for 1 h at room temperature. After washing three times with TBST, the membrane was incubated with alkaline phosphatase-conjugated goat anti-mouse immunoglobulin (Promega). The membrane was washed three times with TBST followed by two brief washes with TBS. The proteins were visualized by using Western Blue stabilized Substrate for alkaline phosphatase (Promega).

2.7. Visualization of GFP fluorescence

Cells were observed with an inverse fluorescence microscope (Olympus IX70) equipped with a FITC filter set, using a ×20 objective for examination of cultures grown on dishes. Fluorescence images were captured using Spot software version 3.0 (Diagnostic Instruments) and Adobe Photoshop version 6.0.

3. Results and discussion

3.1. Features of constructed vectors

Three pET-22b(+)-based and three pET-15b-based vectors were developed for high-level expression and purification of heterologous TAT PTD fusion proteins in *E. coli* (Table 1), and the resultant purified proteins can be further used for the study of protein transduction. As shown in Fig. 1, pETAT-1/2

Table 1
Plasmids constructed in the present study

Plasmid	Host cell	Selection (prok./euk.)	Promoter	TAT PTD	His_6 tag
pETAT-1	P	Amp/none	T7*lac*	WT	C
pETAT-2	P	Amp/none	T7*lac*	M	C
pNB-3	P	Amp/none	T7*lac*	–	C
pETAT-11	P	Amp/none	T7*lac*	WT	N
pETAT-12	P	Amp/none	T7*lac*	M	N
pNB-13	P	Amp/none	T7*lac*	–	N
pHis-TAT-GFP	E	Kan/Neo	CMV/IE	WT	N
pHis-TAT-m-GFP	E	Kan/Neo	CMV/IE	M	N
pHis-GFP	E	Kan/Neo	CMV/IE	–	N

P, prokaryotic; E, eukaryotic; Amp, ampicillin; Kan, kanamycin; Neo, neomycin; CMV/IE, human cytomegalovirus immediate early promoter; WT, wild-type; M, mutation; C, C-terminus; N, N-terminus.

and pETAT-11/12 all contained an N-terminal 11-amino acid TAT PTD or TAT-m for protein intracellular translocation. To enhance the translation initiation of fusion proteins, all the codons encoding TAT peptide were altered to the most preferred ones used in the *E. coli* system. An optional N- or C-terminal His_6 tag allowed in-frame fusion proteins to be readily purified by Ni^{2+} affinity chromatography and detected with anti-His antibody. These vectors also contained a multiple cloning site (MCS) for easy insertion of target genes. Compared with the MCS in their original parental vectors, there was little, if any, modification in pET-22b(+)-based vectors, whereas a few additional cloning sites were added in pET-15b-based vectors. More importantly, not only these added sites in MCS are in-frame with polylinkers in their parental vectors, but also the MCS in pET-15-based vectors and in pET-22b(+)-based vectors are interchangeable. Furthermore, an additional Gly residue was inserted between TAT PTD and MCS for free bond rotation of TAT PTD [7]. Plasmids pNB-3 and pNB-13 were identical to pETAT-1/2 and pETAT-11/12 vectors except for being without TAT PTD and TAT-m.

In addition, three pEGFP-N1-based eukaryotic expression vectors were also developed for studying subcellular localization of TAT PTD hybrid proteins (Table 1). As shown in Fig. 1, a Kozak consensus sequence (GCCACCATGG), embedded with an *Nco*I site and an ATG start codon, was introduced immediately upstream of the His_6 tag to further enhance the translation efficiency of fusion proteins. TAT PTD occurred just upstream of the MCS. The gene of interest can be cloned into MCS to fuse in-frame to TAT PTD and GFP at the C-terminus simultaneously. Using GFP as an indicator has distinct advantages over other detection systems such as antibody detection, which requires both cell fixing and cell killing and often leads to the production of artifacts in the pattern of localization. Most notably, GFP permits a non-invasive localization study in real time using living cells. In case of the non-GFP fusion studies, the GFP gene can be readily removed.

3.2. *High-level expression of TAT fusion proteins in constructed prokaryotic vectors*

To demonstrate the utilities of vectors, several heterogeneous genes including the full-length HSV-TK gene, the enhanced GFP gene, the truncated human Bcl-rambo cDNA fragment (613–1455 bp) and the N-terminally deleted human Smac cDNA fragment (55–717 bp) were cloned respectively into these vectors and expressed in *E. coli* BL21 (DE3) cells (Figs. 2 and 4). Compared with controls, induced proteins were displayed as prominent bands and accounted for approximately 30% of total cellular proteins. As shown in Fig. 2B, *E. coli*-expressed TAT-Bcl-rambo showed a apparent unusual migration with a 20–30-kDa increase, which is not surprising because a similar migration pattern was also observed in mammalian cells by Kataoka et al. [11]. Although the true reason for this retarded migration remains unknown, the possibility of phosphorylation of Bcl-rambo protein cannot be dismissed. It is worthwhile to point out that although the HSV-TK gene failed to be expressed in pNKB-3, it can be highly expressed in pNKB-13 when the His_6 tag is fused to the N-terminus of HSV-TK. It seems unlikely that the expressed HSV-TK was unstable and susceptible to proteolytic degradation. The alternative explanation is that we had observed several rare codons residing in the 5′ end of the HSV-TK coding region, which may eliminate protein translation. The translation barrier is probably overcome by the efficient translation initiation of the His_6 tag as a fusion ahead of HSV-TK [17]. Additionally, while expressed Bcl-rambo and GFP were found mostly in soluble form, expressed HSV-TK and Smac/DIABLO, whether fused with or without TAT PTD, remained largely in inclusion bodies (data not shown), suggesting that the status of solubility is dependent on the intrinsic properties of the protein itself.

3.3. *TAT-Smac is able to enter cultured A549 cells*

To test the capability of transduction for TAT PTD, *E. coli*-expressed Smac fusion proteins with or without TAT PTD were purified under native conditions as described in Section 2. TAT-Smac and Smac were added directly to the cultured A549 cells at a final concentration of 400 nM, and treated cells were harvested at indicated time points followed by Western analysis. We also incubated A549 cells with TAT-Smac and Smac at various concentrations for 3 h and levels of transduced proteins were analyzed by Western blot. As shown in Fig. 3, TAT-Smac translocation into A549 cells was time- (Fig. 3A) and dose- (Fig. 3B) dependent. TAT-Smac was detected only in the lysate pellet but not in the lysate supernatant, indicating that TAT-Smac probably existed in the nucleus. In contrast, Smac without TAT PTD could not be detected either in the pellet or in the supernatant (data not shown). To further examine whether transduced TAT-Smac still retains its pro-apoptotic activity, the MTT cell death assay was performed. As shown in Fig. 3C, A549 cells incubated with TAT-Smac (200 nM) in the presence of taxol (100 nM) showed considerable cell death (45%), when compared with cells treated with Smac lacking the TAT PTD (200 nM), which gave rise to 30% of cell death. The relatively higher background cell death may be attributed to the toxicity

A

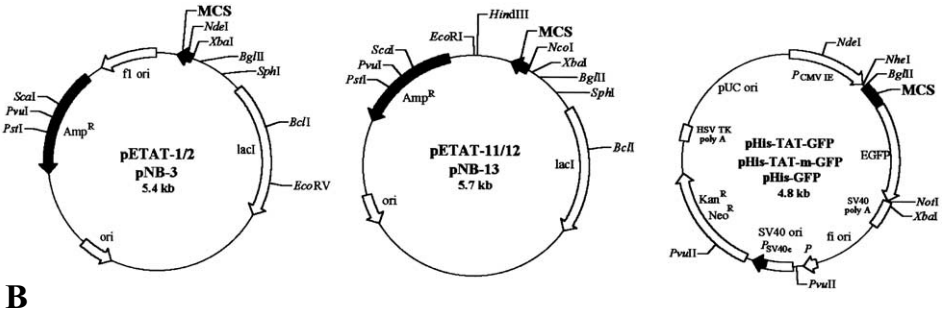

B

pNB-3

5′…CAT**ATG**GGTACCTCGGATCCGAATTCGAGCTCCGTCGACAAGCTTGCGGCCGCAC
***Nde*I *Kpn*I *Bam*HI *Eco*RI *Sac*I *Sal*I *Hin*dIII *Not*I**
***Eag*I**

TCGAGCACCACCACCACCACCAC **TGA**AGA…3′
***Xho*I**
***Ava*I**

pNB-13

5′…ACC**ATG**GGCAGCAGCCATCATCATCATCATCACAGCAGCGGCCTGGTGCCGCGCG
*Nco*I

GCAGCCATATGGGTACCTCGGATCCGAATTCGAGCTCCGTCGACAAGCTTGCGGCCGC
***Nde*I *Kpn*I** *Bam*HI *Eco*RI ***Sac*I *Sal*I** *Hin*dIII ***Not*I**

ACTCGAGGATCCGGCTGCTAACAAAGCCCGAAAGGAAGCTGAGTTGGCTGCTGCCAC
***Xho*I** *Bam*HI

CGCTGAGCAA**TAA**CTA…3′

pHis-GFP

5′…CTCAGATCTGCCACC**ATG**GGCAGCAGCCATCATCATCATCATCACAGCAGCGGCCT
*Bgl*II *Nco*I

GGTGCCGCGCGGCAGCCATATGGGTACCCTCGAGCTCAAGCTTCGAATTCTGCAGTCG
*Nde*I *Kpn*I ***Xho*I *Sac*I *Hin*dIII *Eco*RI *Pst*I *Sal*I**
***Acc*I**

ACGGTACCGCGGGCCCGGGATCCACCGGTCGCCACCATGGTG…3′
*Kpn*I **SacII *Apa*I *Xma*I *Bam*HI *Age*I**
***Sma*I**

pETAT-1/11 and pHis-TAT-GFP

5′…ATG**TACGGTCGTAAAAAACGTCGTCAGCGTCGTCGT**GGT…3′

pETAT-2/12 and pHis-TAT-m-GFP

5′…ATG**TACGCTCGTGCTGCTGCTCGTCAGGCTCGTGCT**GGT…3′

Fig. 1. Schematic maps of vectors (A) and nucleotide sequences present in the cloning/expression regions (B). ATG start codon and stop codons are shown in bold. The underlined sequence represents the Kozak consensus sequence. The shaded sequence indicates the His_6 tag. The boxed sequence denotes the variable region. The boxed nucleotide sequences for TAT and TAT-m are shown in bold. Unique sites located in MCS are shown in bold. The *Bam*HI sites in pET-15b-based vectors and the *Kpn*I sites in pEGFP-N1-based vectors can also be used for the insertion of DNA fragments into these vectors.

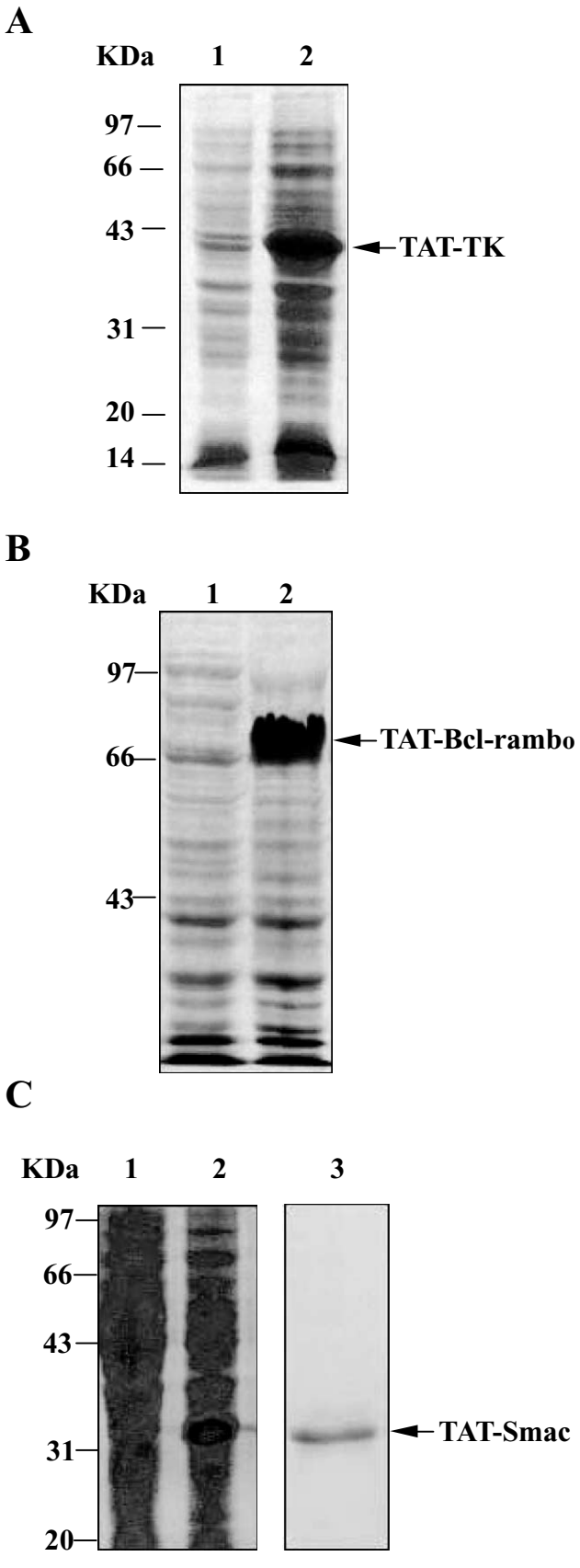

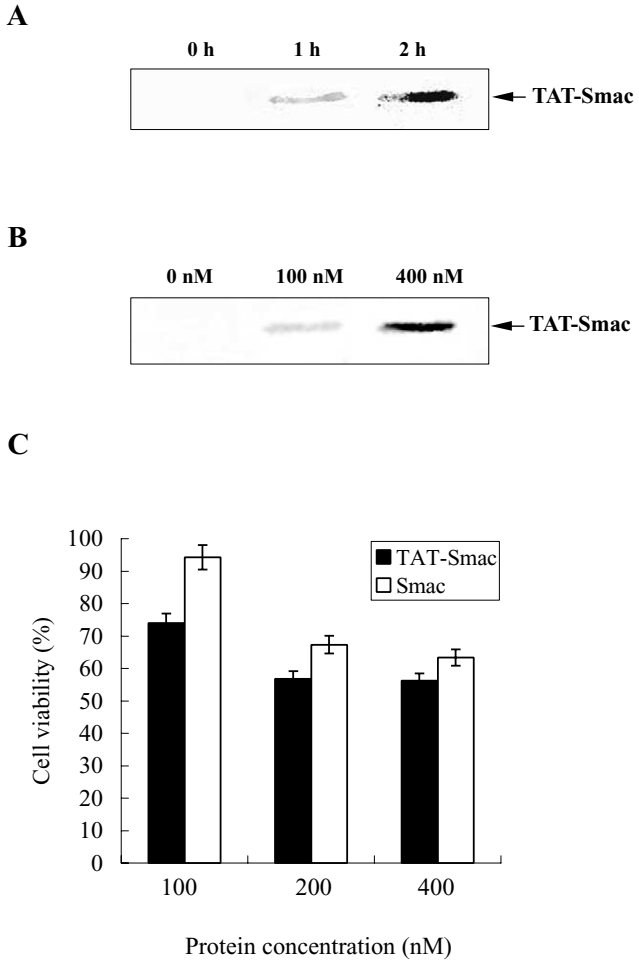

Fig. 3. Transduction of TAT-Smac fusion protein into cultured A549 cells in a time- (A) and dose- (B) dependent manner. TAT-Smac (400 nM) was added to A549 culture media for 0, 1 and 2 h. A549 cells were treated with 0, 100 and 400 nM of TAT-Smac for 3 h. The lysate pellet fractions were analyzed by Western blot. Molecular size of protein is indicated on the left. C: Transduced TAT-Smac promoted cell death. A549 cells was incubated with TAT-Smac or Smac for 6 h at final concentrations of 100, 200 and 400 nM, followed by induction of taxol at a final concentration of 100 nM for an additional 10 h. Cell death effects were assessed by the MTT assay. The effect of cell death was normalized as a percentage using cells treated with taxol alone as control.

of exogenously added Smac. The result that transduced TAT-Smac did not yield remarkable cell death was not unexpected, since Smac/DIABLO by itself is a weak pro-apoptotic factor, it can only potentiate apoptosis induced by diverse stimuli. Thus we have demonstrated that transduced TAT-Smac was able to promote taxol-induced cell death.

←

Fig. 2. Expression and purification of TAT fusion proteins in *E. coli*. A: Expression of TAT-TK with pNKB-1. Lane 1, uninduced; lane 2, induced. B: Expression of TAT-Bcl-rambo using pETAT-1 as a vector. Lane 1, uninduced; lane 2, induced. C: Expression and purification of TAT-Smac using pETAT-1 as a vector. Lane 1, uninduced; lane 2, induced; lane 3, purified TAT-Smac. Molecular size of protein is indicated on the left.

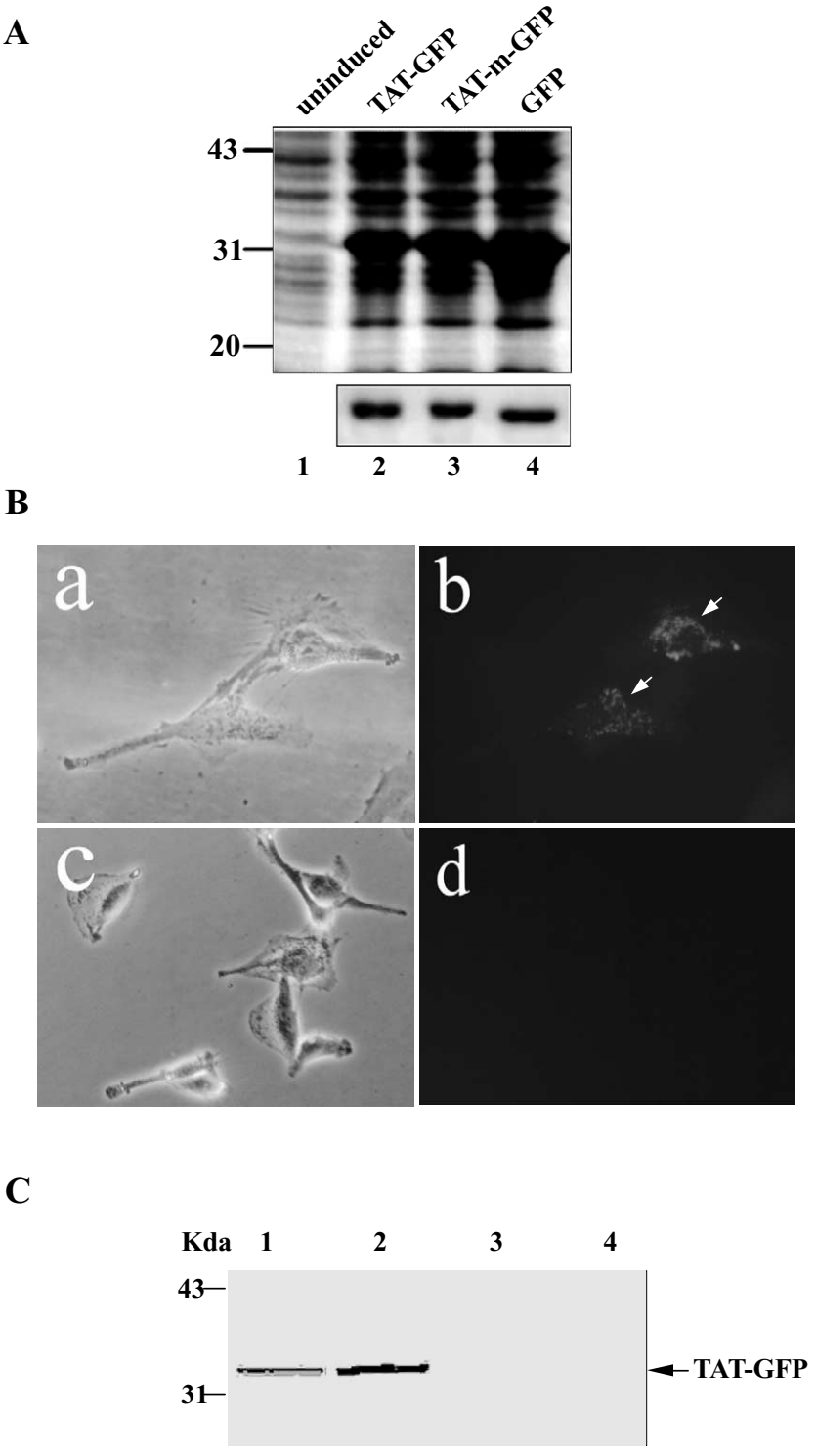

Fig. 4. Transduction of *E. coli*-expressed TAT-GFP fusion protein into mammalian cells and its subcellular localization. A: Expression and purification of GFP with or without TAT PTD in *E. coli*. Upper panel: lane 1, uninduced control; lane 2, induced TAT-GFP; lane 3, induced TAT-m-GFP; lane 4, induced GFP. Purified TAT-GFP, TAT-m-GFP and GFP are shown in the lower panel. B: Phase contrast images (a and c) and corresponding fluorescence micrographs (b and d) of transduced TAT-GFP (a and b) or GFP (c and d) in A172 cells. a,b, denatured TAT-GFP; c,d, denatured GFP. Arrows denote transduced TAT-GFP within the cells. C: Western blot of transduced TAT-GFP fusion proteins. Both denatured and native TAT-GFP or GFP controls at a final concentration of 500 nM were added to cultured A172 cells for 12 h followed by Western blot analysis. Lane 1, native TAT-GFP; lane 2, denatured TAT-GFP; lane 3, native GFP; lane 4, denatured GFP. Molecular size of protein is indicated on the left.

3.4. *E. coli-expressed TAT-GFP, but not GFP is capable of transducing into cells*

To further examine the usefulness of these vectors and the synthetic TAT PTD, the enhanced GFP gene fragment from pEGFP-N1 was subcloned into vectors pETAT-11, pETAT-12 and pNB-13 and expressed in *E. coli* BL21 (DE3) cells (Fig. 4A). We found these fusion proteins could be well expressed even without IPTG induction. The fusion proteins could be easily monitored by its green fluorescence during the entire protein expression and purification process. To take advantage of the convenience of direct visualization of GFP fusion proteins, we tested whether *E. coli*-expressed proteins from our constructed vectors were able to transduce into the mammalian cells. We incubated A172 cells with denatured TAT-GFP and GFP control respectively and the results are shown in Fig. 4B. Twelve hours after incubation, TAT-GFP could be clearly detected within the A172 cells, indicating TAT-GFP was capable of transducing into mammalian cells. In addition, the transduced TAT-GFP was found to be mainly located in the cytosol but not in the nucleus (Fig. 4B, a,b). In contrast, GFP control could not be detected in these cells (Fig. 4B, c,d), suggesting the TAT PTD is required for protein transduction. We also performed protein transduction using soluble TAT-GFP, and similar results were obtained (data not shown), indicating that the folding state of TAT-GFP might not be very critical for its protein translocation. The successful transduction was further confirmed by Western blot analysis (Fig. 4C). Both native TAT-GFP (lane 1) and denatured TAT-GFP (lane 2) can be detected from total A172 cell lysates, whereas GFP control in either of two forms was absent in A172 cell lysates (lanes 3 and 4).

Thus far, subcellular distribution of TAT-GFP still remains controversial. Caron et al. [18] had reported that there was no visible nuclear localization to be detected when denatured TAT-eGFP protein was added into cultured muscle cells, whereas Choi's group [19] demonstrated that Tat (residues 49–57)-GFP fusion protein was able to distribute in both the nucleus and the cytoplasm of *Drosophila* S2 cells. Our results from TAT-GFP transduction in A172 cells are in good agreement with those of Caron et al. These two different observations may be explained by the fact that nuclear localization is a complicated event influenced by many factors such as the fine structure of TAT PTD, denaturing and purification conditions, folding state of TAT fusion polypeptides and the host cell type.

3.5. *TAT PTD is sufficient to confer nuclear localization and nucleolar accumulation in transfected mammalian cells*

To test the production of GFP fusion proteins with our eukaryotic expression vectors, HEK293T cells were transfected with pEGFP-N1, pHis-TAT-GFP, pHis-TAT-m-GFP and pHis-GFP. Forty-eight hours after transfection, cells were harvested, lysed and subjected to SDS–PAGE followed by Western blot analysis. As shown in Fig. 5, all the fusion proteins were overexpressed with expected molecular weights. It is noteworthy, however, that a faint band with the molecular weight of GFP can be detected in each lane. Although a Kozak sequence was introduced immediately upstream of the coding sequence in these vectors, the possibility that another putative Kozak sequence and ATG start codon of GFP itself may also serve as a weak translational initiator cannot be excluded (see Fig. 1).

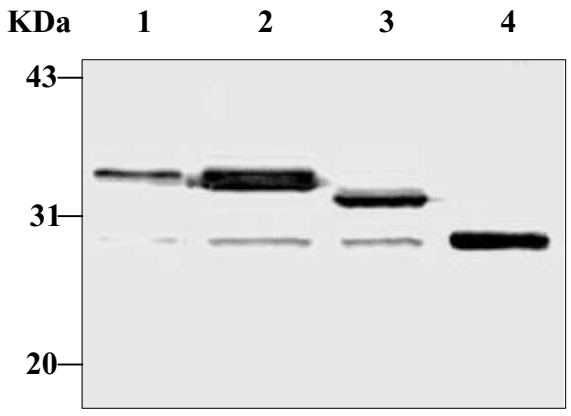

Fig. 5. Expression of TAT-GFP fusion proteins in mammalian cells. HEK293T cells were transiently transfected with 1 μg of various mammalian expression constructs. At 48 h post-transfection, cell lysates were subjected to Western blot analysis. Lane 1, pHis-TAT-GFP; lane 2, pHis-TAT-m-GFP; lane 3, pHis-GFP; lane 4, pEGFP-N1. Molecular size of protein is indicated on the left.

To assess the subcellular localization of TAT PTD, plasmids encoding GFP, His-TAT-GFP, His-TAT-m-GFP and His-GFP were transiently transfected into A549 cells. At 48 h post-transfection, the GFP fusion protein expression patterns were examined in living cells directly under a fluorescence microscope. The GFP from the control vector pEGFP-N1 was found throughout cells in a diffuse cytoplasmic and nuclear pattern (data not shown). In sharp contrast, His-TAT-GFP was predominantly located in the nucleus and accumulated in the nucleolus, resulting in a very weak fluorescence in the cytoplasm (Fig. 6A). Addition of a His_6 tag to the N-terminus of GFP also yielded a diffuse fluorescence throughout the cells, quite similar to GFP control protein (Fig. 6B).

To further determine whether TAT PTD-mediated nuclear localization was only restricted to A549 cells, monkey kidney COS-7 cells (Fig. 6C,D) were transfected with the same plasmids used for A549 cells. Consistent with the observation obtained from A549 cells, TAT-GFP fusion protein expressed in COS-7 cells displayed efficient nuclear and nucleolar importation. Some other cell lines including HeLa, A172 and HEK293T were also tested for nuclear targeting by TAT PTD, and similar results were obtained (data not shown). The expression in all these cells was allowed to continue for up to 48 h and the GFP fluorescence was monitored periodically, but no visible changes in expression pattern were observed.

Our results clearly demonstrate that TAT-GFP expressed in mammalian cells was located predominantly in the nucleus, and the majority was sequestered within the nucleolus. This finding was consistent with previous observations that GFP fused to full-length TAT protein resulted in nuclear/nucleolar localization by using a transfection system [20] and also was quite similar to the results reported by Vivès et al. using TAT PTD-mediated protein transduction [6]. We observed very faint cytoplasmic fluorescence present within the cells tested. Currently we are not certain whether this represents a truly cytoplasmically localized TAT-GFP or is the basal level expression resulting from a leaky expression of GFP protein per se (see above). We believe that transfected expression and localization of TAT PTD fusion protein might be more reli-

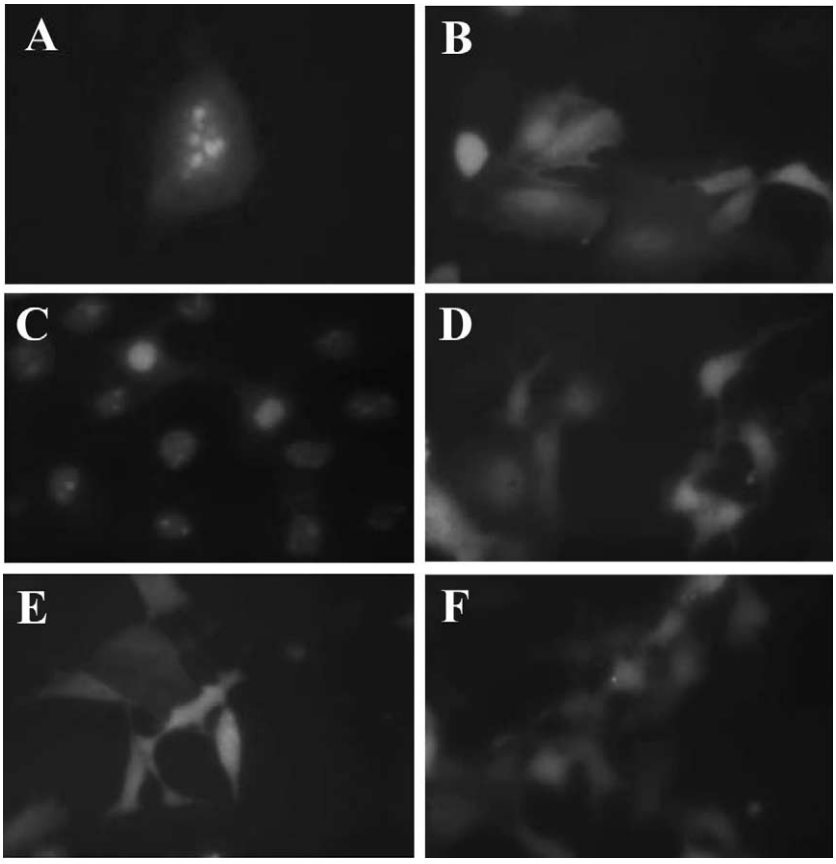

Fig. 6. Subcellular localization of TAT-GFP in transfected mammalian cells. A549 cells (A,B,E) and COS-7 cells (C,D,F) were transiently transfected with 1 μg of plasmids pHis-TAT-GFP (A,C), pHis-GFP (B,D) and pHis-TAT-m-GFP (E,F). At 48 h after transfection, the fluorescence images (20× objective) were captured under the fluorescence microscope using Spot software.

able since subcellular compartment distribution of proteins expressed within the cells has higher fidelity compared with transduced proteins expressed in *E. coli*.

To examine whether the TAT-GFP fusion proteins extracted from transfected mammalian cells could re-transduce into a fresh cell monolayer, we extracted TAT-GFP from transfected HeLa cells using the high-salt lysis buffer described by Elliott et al. [21] and/or by sonication; the detection of fluorescence in fresh cultured cells was unsuccessful when the transfected cell extract was exogenously added to culture media. This result was not unexpected, since TAT PTD, unlike VP22, is unable to confer its shuttling capacity of exporting from the primary transfected cells and re-entering the surrounding cells [5,20,22].

3.6. *Mutant TAT peptide abolishes its ability of nuclear targeting*

To assess whether the mutations within TAT PTD could affect its capability of translocation and/or subcellular localization, we substituted six out of 11 amino acids within the TAT peptide. Basic amino acids (K and R) were changed to the neutral amino acid alanine (A). Most changes took place in the putative NLS region GRKKRR which now became ARAAAR. The proposed protein translocation region RRR was changed to ARA. This mutant variant TAT-m was previously reported to possess enhanced protein transduction potential compared with the model structure TAT PTD [10]. However, in our hands we did not find that mutant TAT-m was superior to the wild-type TAT PTD in terms of leading the proteins to translocate across the cell membrane. To test whether *E. coli*-expressed TAT-m-GFP was also able to efficiently transduce into mammalian cells, TAT-m-GFP in either denatured or native form was exogenously added to A172 cell culture medium, and green fluorescence can only be barely detected. This may be explained by the fact that the six-amino acid substitution within the TAT PTD compromised its ability to transduce into these particular A172 cells. In sharp contrast to the nuclear/nucleolar localization of His-TAT-GFP, ectopically expressed His-TAT-m-GFP markedly abolished its ability to nuclear localization (Fig. 6E,F), indicating the functional significance of these basic amino acids.

In summary, we have successfully constructed a series of prokaryotic and eukaryotic expression vectors for the purpose of protein transduction and subcellular localization. Their utilities have been tested by cloning and overexpression of the genes encoding HSV-TK, Bcl-rambo, Smac/DIABLO and GFP. The subcellular location of TAT or TAT-m was assessed by generation of corresponding GFP fusion proteins. The main features of these constructed vectors are (1) utilization of an 11-amino acid HIV-1 TAT PTD for efficient protein transduction and subcellular localization, (2) most favorable codons chosen for TAT peptide for elevated translation initiation, (3) an additional Gly residue was introduced to aid free bond rotation of TAT PTD, (4) addition of a His_6 tag greatly facilitates purification and detection, (5) interchangeable MCS cassettes used for selection of cloning vectors, (7)

enhanced GFP used as a visible indicator for quickly monitoring eukaryotic expression and subcellular location, (8) mutant TAT-m lacking NLS restricts the expressed proteins to enter the nucleus. We believe that our constructed expression vectors are ideally suited for high-level expression of foreign genes and efficient transduction of exogenously added proteins. Many important researches rely on the gene products to be localized at correct subcellular compartment(s) in order to acquire their optimal activities. We believe our vectors may provide useful tools to deliver therapeutic proteins into mammalian cells.

Acknowledgements: We thank Dr. Steven F. Dowdy for his helpful suggestions and comments on this study, Dr. Nicolas J. Caron for his constructive advice on protein transduction techniques. These vectors and more detailed information about the constructions are available from the authors on request. This work was supported by Key Project Fund (KSCX2-2-01-004) and a special grant (to M.W.) from the Chinese Academy of Sciences, a grant from the Chinese National Science Foundation, and a grant from the Natural Science Foundation of Anhui Province (01043702).

References

[1] Green, M. and Loewenstein, P.M. (1988) Cell 55, 1179–1188.
[2] Frankel, A.D. and Pabo, C.O. (1988) Cell 55, 1189–1193.
[3] Schwarze, S.R., Hruska, K.A. and Dowdy, S.F. (2000) Trends Cell Biol. 10, 290–295.
[4] Wadia, J.S. and Dowdy, S.F. (2002) Curr. Opin. Biotechnol. 13, 52–56.
[5] Ford, K.G., Souberbielle, B.E., Darling, D. and Farzaneh, F. (2001) Gene Ther. 8, 1–4.
[6] Vivès, E., Brodin, P. and Lebleus, B. (1997) J. Biol. Chem. 272, 16010–16017.
[7] Nagahara, H., Vocero-Akbani, A.M., Snyder, E.L., Ho, A., Latham, D.G., Lissy, N.A., Becker-Hapak, M., Ezhevsky, S.A. and Dowdy, S.F. (1998) Nature Med. 4, 1449–1452.
[8] Ruben, S., Perkins, A., Purcell, R., Joung, K., Sia, R., Brghoff, R., Hasetine, W.A. and Rosen, C.A. (1989) J. Virol. 63, 1–8.
[9] Hauber, J., Malim, M.H. and Cullen, B.R. (1989) J. Virol. 63, 1181–1187.
[10] Ho, A., Schwarze, R., Mermelstein, S.J., Waksman, G. and Dowdy, S.F. (2001) Cancer Res. 61, 474–477.
[11] Kataoka, T., Holler, N., Micheau, O., Martinon, F., Tinel, A., Hofmann, K. and Tschopp, J. (2001) J. Biol. Chem. 276, 19548–19554.
[12] Du, C.Y., Fang, M., Li, Y.C., Li, L. and Wang, X.D. (2000) Cell 102, 33–42.
[13] Verhagen, A.M., Ekert, P.G., Pakusch, M., Silke, J., Connolly, L.M., Reid, G.E., Moritz, R.L., Simpson, R.J. and Vaux, D.L. (2000) Cell 102, 43–53.
[14] He, T.C., Zhou, S., Costa, L.T.D., Yu, J., Kinzler, K.W. and Vogelstein, B. (1998) Proc. Natl. Acad. Sci. USA 95, 2509–2514.
[15] Becker-Hapak, M., McAllister, S.S. and Dowdy, S.F. (2001) Methods 24, 247–256.
[16] Kwon, H.Y., Eum, W.S., Jang, H.W., Kang, J.H., Ryu, J., Lee, B.R., Jin, L.H., Park, J. and Choi, S.Y. (2000) FEBS Lett. 485, 163–167.
[17] Hare, D.L., Sadler, J.R. and Betz, J.R. (1984) Gene 32, 117–128.
[18] Caron, N.J., Torrente, Y., Camirand, G., Bujold, M., Chapdelaine, P., Leriche, K., Bresolin, N. and Tremblay, J.P. (2001) Mol. Ther. 3, 310–318.
[19] Han, K., Jeon, M-J., Kim, K-A., Park, J. and Choi, S.Y. (2000) Mol. Cells 10, 728–732.
[20] Stauber, R. and Pavlakis, G.N. (1998) Virology 252, 126–136.
[21] Elliott, G. and O'Hare, P. (1997) Cell 88, 223–233.
[22] Schwarze, S.R. and Dowdy, S.F. (2000) Trends Pharmacol. Sci. 21, 45–48.